32 x 32 Geiger-mode LADAR cameras

Ping Yuan*, Rengarajan Sudharsanan, Xiaogang Bai, Joseph Boisvert, Paul McDonald, and Eduardo Labios
Spectrolab Inc., a Boeing Company, 12500 Gladstone Ave., Sylmar, CA, USA 91342

Michael S Salisbury, Gary M Stuart, Harrison Danny, Angel A Portillo, and Alric B Roybal
Boeing SVS Inc, 4411 The 25 Way NE # 350, Albuquerque, NM 87109

Stephen Van Duyne, Greg Pauls, and Stephen Gaalema
Black Forest Engineering, LLC, 1879 Austin Bluffs Parkway, Colorado Springs, CO 80918

ABSTRACT

For the wide applications of LAser Detection and Ranging (LADAR) imaging with large format Geiger-mode (GM) avalanche photodiode (APD) arrays, it is critical and challenging to develop a LADAR camera suitable to volume production with enough component tolerance and stable performance. Recently Spectrolab and Black Forest Engineering developed a new 32x32 Read-Out Integrated Circuit (ROIC) for LADAR applications. With a specially designed high voltage input protection circuit, the ROIC can work properly even with more than 1 % of pixels shorted in the APD array; this feature will greatly improve the camera long-term stability and manufacturing throughput. The Non-uniform Bias circuit provides bias voltage tunability over a 2.5 V range individually for each pixel and greatly reduces the impact of the non-uniformity of an APD array. A SMIA high speed serial digital interface streamlines data download and supports frame rates up to 30 kHz. The ROIC can operate with a 0.5 ns time resolution without vernier bits; 14 bits of dynamic range provides 8 µs of range gate width. At the meeting we will demonstrate more performance of this newly developed 32x32 Geiger-mode LADAR camera.

1. INTRODUCTION AND BACKGROUND

The recent progress in the short wavelength infrared region (SWIR) three-dimension imaging provides an important solution for foliage penetration, camouflage imaging, and aerial mapping in battlefield intelligence and Earth survey. Its airborne applications, which make the most potential market for this technology, have posted a series of challenges to the camera. Because the laser and its service system take most of the weight, power, and volume of a LADAR system, it is critical to maximize the camera sensitivity to reduce the laser power requirement in order to enhance the ranging distance and reduce the weight, power and volume of the whole system. InP-based single-photon counting GM-APDs fit excellently to this requirement. Geiger-mode avalanche photodiode focal plane arrays (GM-FPAs) have been reported by both MIT Lincoln Laboratory[1] and Boeing Spectrolab[2] for SWIR applications. Due to the availability of high power emitters, most of the effort to date has been focused on photodiodes operating at 1.06 µm. Important figures-of-merits for GM-APDs include dark count rate (DCR) and photon detection efficiency (PDE) which together establish the upper limit of the signal-to-noise ratio for the entire sensor system. For active 3-D imaging, sensor's FPA timing jitter and crosstalk are also critical because the jitter sets the upper limit of range resolution while the latter greatly influences the spatial resolution. Frame rate limits the sensor update time which is also a critical performance parameter in airborne applications. Since it is primarily determined by the data process and download rate, the GM-APD afterpulsing, or temporal crosstalk between range gates, is normally not a great concern in imaging applications as long as it is no less than 100 kHz. Other important parameters include weight, power, and volume. Because most of the power consumed in a LADAR camera is by the thermoelectric coolers (TEC), a higher APD operation temperature is always welcome to airborne applications.

* Email: ping.yuan@boeing.com; Tel: 818 898 7578; Fax : 818 838 7474.

Laser Radar Technology and Applications XV, edited by Monte D. Turner, Gary W. Kamerman,
Proc. of SPIE Vol. 7684, 76840C · © 2010 SPIE · CCC code: 0277-786X/10/$18 · doi: 10.1117/12.851525

Spectrolab and Black Forest Engineering have been working under a DARPA Elusive Surface Target Engagement Technology program to advance the performance of both the avalanche photodiode detector and ROIC arrays that together comprise an FPA. Black Forest Engineering has designed a new 32x32 ROIC with enhanced capabilities that include: a non-uniform bias (NUB) correction that can be applied to individual pixels across the array; and a modified pixel input circuit that effectively removes high dark current (shorted) APD pixels from the array to reduce the overall current draw that would otherwise cause an FPA to fail. Spectrolab has introduced a feature to the APD detector array that reduces the optical crosstalk between pixels to <0.05% and reduces Dark Count Rate (DCR) at operating temperature to <20 kHz. External PDE on detectors alone, without a microlens, in excess of 40% has been demonstrated for reverse-illuminated arrays.

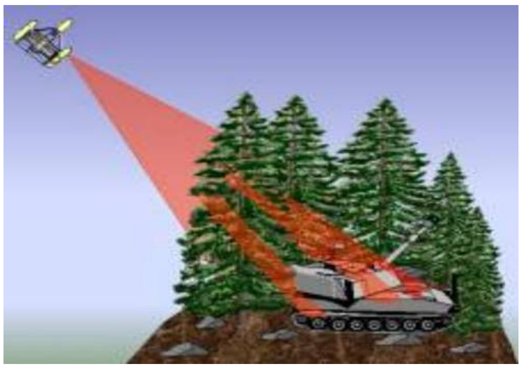

(A) Foliage penetration

(B) Aerial mapping

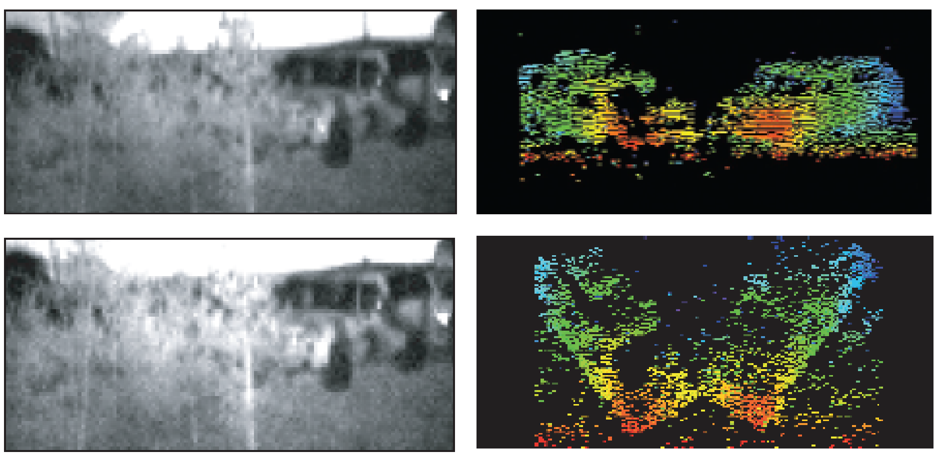

(C) Camouflage imaging

Figure 1. Airborne applications for 3-D imaging.

All these parameters mentioned above must be optimized for the optimal sensor performance. In practice these parameters are not decoupled and often trade off against one another. A robust FPA read out integrated circuit (ROIC) can improve sensor performance by mitigating APD deficiencies. However, an FPA design is fundamentally limited by detector performance. Table 1 lists the most important FPA figures of merit that impact single photon counting sensor systems.

Parameter	Spec	Test conditions
Wavelength	1.06 µm	
Format	32x32	
Pixel Pitch	100 µm	
PDE	40%	240K, 4V overbias
Fill Factor	70%	
DCR	20 kHz	240K, 4V overbias
Cross talk	<1%	Optimized overbias for SCA
Pixel operability	99%	
RMS timing jitter	0.5 ns	

Table 1. Typical single photon counting focal plane array figures-of-merits for a 32x32 GM-APD array presently fabricated at Spectrolab.

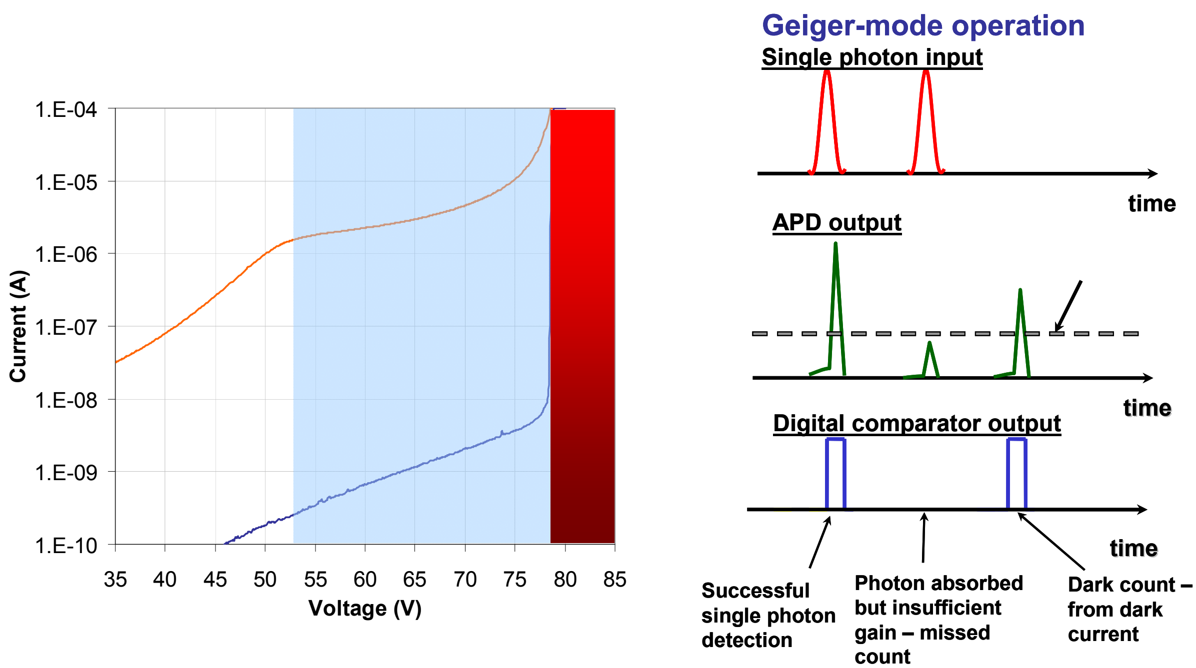

Figure 2. Geiger-mode operation of an avalanche photodiode. The left panel shows the typical IV characteristics of a 200 um GM-APD under illumination and in dark. The linear mode region is highlighted in blue, while the Geiger-mode operation region is shaded in red. The right panel illustrated the three possible cases in Geiger-mode detection.

2. GM-APD FPA FUNDAMENTALS

In Geiger-mode operation the avalanche photodiodes are biased above the breakdown voltage, ~ 2-4 V, for a short period of time during which the sensor is active. If a photon in the sensitive spectrum falls on the detector pixel in this period, it has a probability to be absorbed and multiplied in the GM-APD such that the amplitude of the result pulse is large enough to be converted into a digital pulse that can be registered by the following readout circuit. This probability is a figure-of-merit called photon detection efficiency (PDE). Due to various carrier generation mechanisms in GM-APDs, there is still some probability for the pixels to generate some output pulses even without any incident photons. This probability is characterized by dark count rate (DCR) and it represents the noise of GM-APD arrays. Typically DCR increases with overbias and operating temperature. Because a higher overbias also yields a better PDE, for a better signal-to-noise ratio, the trade-off between PDE and DCR has to be carefully considered in the device operation point selection. Figure 2 details the general concepts of Geiger-mode operation.

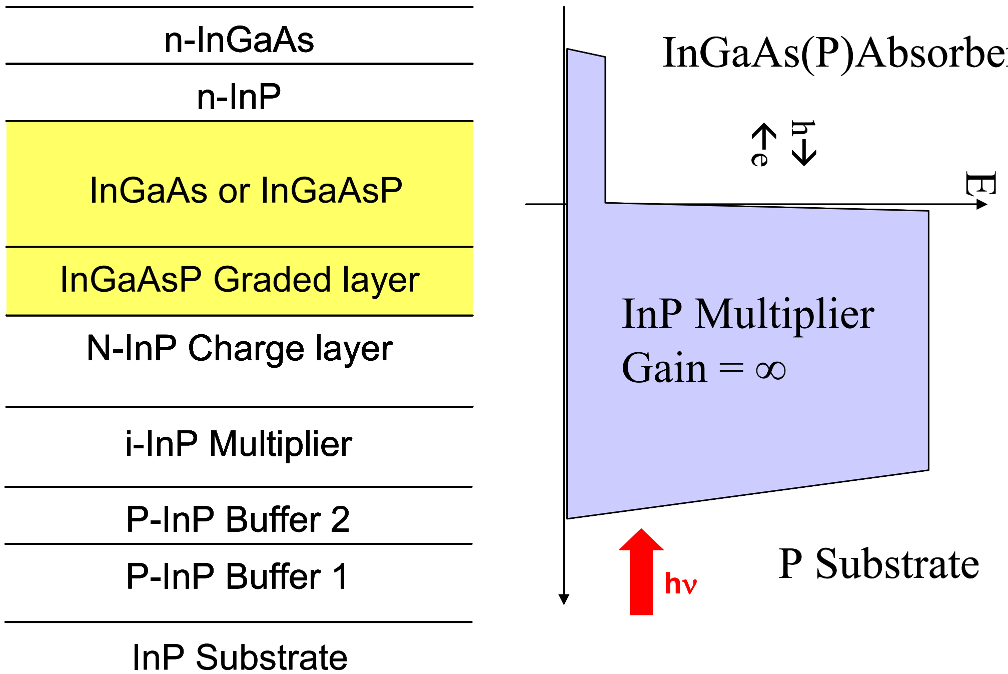

Figure 3. 1.06 μm GM-APD device design and resultant electric field profile during operation.

Figure 3 shows the InGaAsP/InP GM-APD separate absorption and gain and multiplication (SAGM) device structure for 1.06 μm operation. The multiplication layer and silicon doped charge layer are both formed with InP. An InGaAsP alloy is used in the absorption layer for 1.06-μm photons. The right panel shows the electric field profile at operation in this device structure. With a carefully controlled charge layer, the electric filed in the multiplier is high for appreciable avalanche gain and it is low across the absorption layer to prevent tunneling of carrier so that the DCR is low in these devices. The top N^+ InGaAs layer is used as a contact layer. The nominal thickness the InGaAsP absorption layer is 1.5 μm for good quantum efficiency. The device growth and characterization details have been described in previous literatures[2].

3. SINGLE DEVICE PERFORMANCE

As described earlier[2], single element mesa devices with different mesa diameters, from 20 μm to 200 μm, are fabricated to evaluate the quality of epitaxial wafers. Initial I-V testing is done at room temperature to determine the breakdown voltage, punch through voltage, and leakage current. The device optical gain and responsivity were measured by illuminating with a 1.06 μm wavelength laser. The left panel of Figure 2 shows the dark current and gain versus bias characteristics of a 200 μm diameter device. The bulk current density referred to unity gain is a typical figure of merit for APDs and in this case $J_D(M=1)=630\ nA/cm^2$. One of the most important figure-of-merits of GM APDs is DCR. Figure 4 shows the average DCR versus temperature at 4 V overbias collected on 30-µm pixels from three APD arrays[3], which are the representatives of three generations of 1.06 µm APD arrays fabricated at Spectrolab over the last few years. As reported by Lincoln Laboratory[4] and analyzed by Spectrolab[3], significantly lower DCR can be achieved with a thicker multiplication layer due to the reduced electric field in the multiplication region. However, a thicker multiplier inevitably results in higher breakdown voltage. In practice, our trade-off point of the multiplier thickness is about 1.5 um. Another important improvement involves replacing the original n-type substrates with p-type ones to grow the n-on-p APD junction. This substrate change removes a parasitic forward biased p-n junction at the bottom of the device structure and reduces the DCR substantially. With all these improvements, the DCR of a 30-µm-diameter GM-APD pixel can be less than 1 kHz at 240 K and 4V overbias.

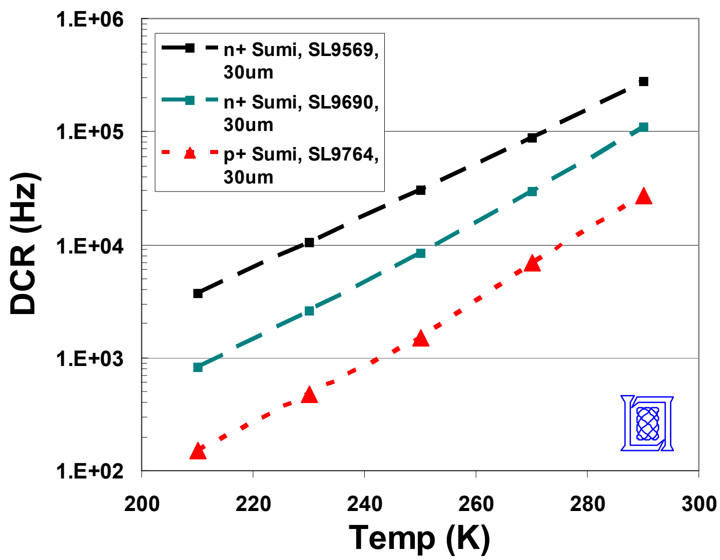

Figure 4. DCR as a function of temperature of three typical Spectrolab 30 µm diameter Geiger-mode APD pixels. These data were measured at MIT Lincoln Laboratory.

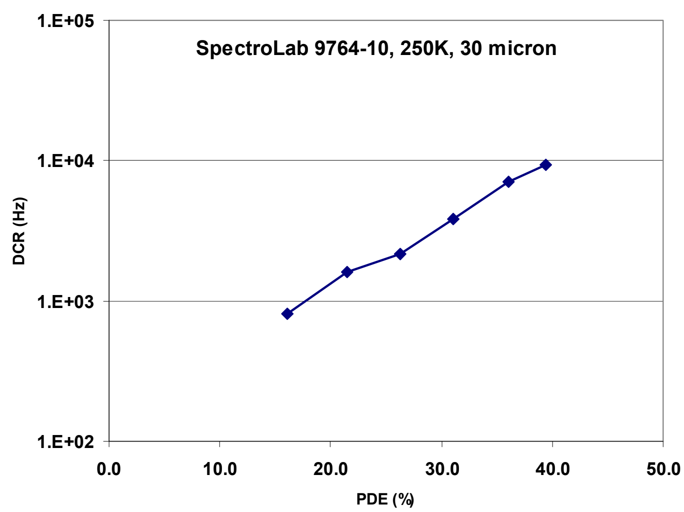

Figure 5. The DCR vs PDE at 250 K. The measurement was taken on a 30-µm diameter InGaAsP/InP APD optimized for 1.06 µm operation.

The ultimate performance tradeoff of GM-APD is between DCR and PDE. Figure 5 shows the PDE-vs-DCR curve of our 30-um-diameter GM-APD on P+ InP substrate at 250 K measured at various overbias. These data were taken on bare pixels and do not include the optical losses due to a microlens array, which is subsequently affixed to the APD detector chip for a better field factor. Based on this measurement, 40% of PDE can be achieved with a DCR budget of 10 kHz. Due to the free carrier absorption of the P+ InP substrate[5], GM-APD arrays being presently fabricated at Spectrolab are being grown on p- substrates and 20-30 % improvement in PDE is expected.

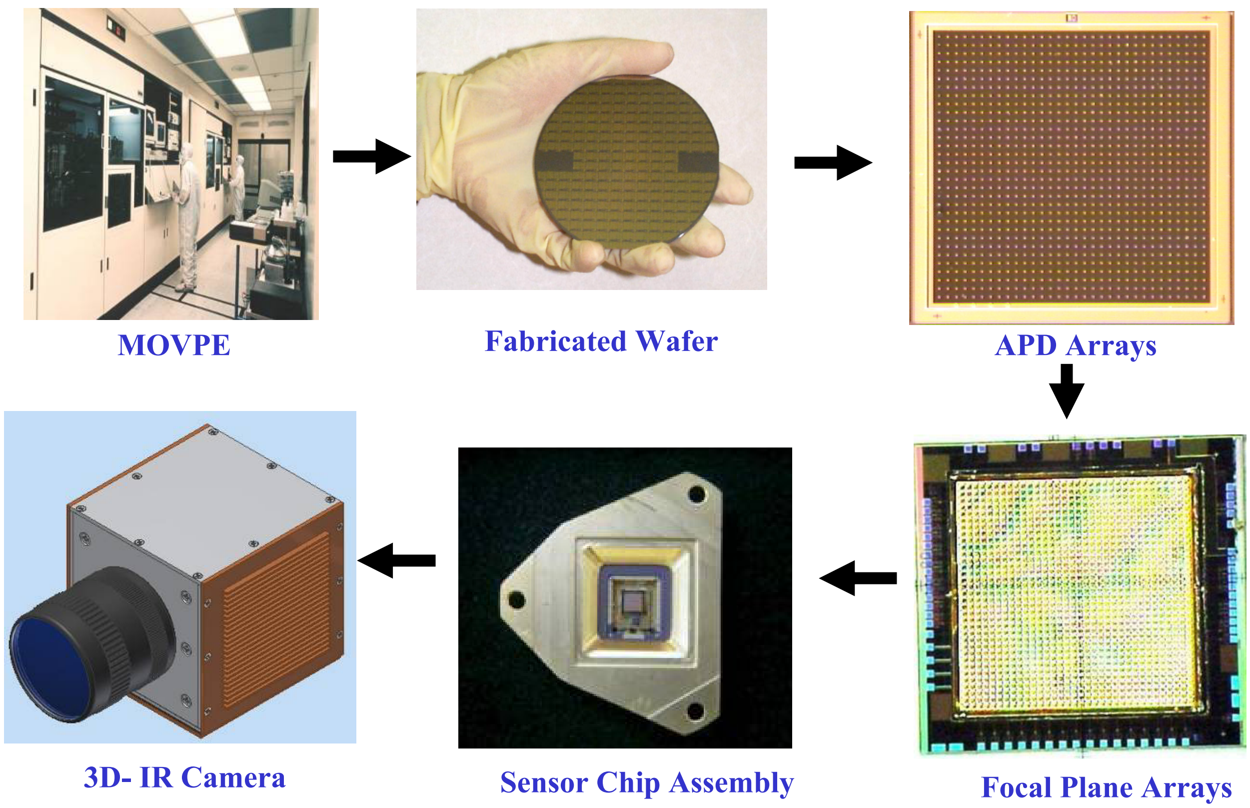

Figure 6. Vertical integration of camera fabrication at Spectrolab.

4. SPECTROLAB GEN-I LADAR CAMERA

With extensive capacities in MOVPE epitaxy, wafer process, and module packaging, Spectrolab vertically integrated the LADAR camera manufacturing in house. Figure 6 shows the pictures of several key components in the process in building the camera. After the detector array fabrication, Indium bumps were evaporated on to the array pixels. The detector array with indium bumps was integrated with a CMOS 2002 readout-integrated circuit (ROIC) designed by MIT-LL by flip-chip bonding. A GaP microlens array was mechanically attached to the focal plane array for a better fill factor after this flip-chip process. Then, as shown in Figure 7, the focal plan array (FPA) was mounted on to a two-stage TE cooler and wire bonded to a 69 pin grid array. Later, the package was hermetically sealed with an AR-coated sapphire window into a sensor chip assembly (SCA). Finally, the SCA was assembled with a data acquisition card and a second TE-cooler and built into a LADAR camera.

Figure 8 shows the pictures, block diagram, and controlling graphical user interface (GUI) of Spectrolab Gen-I LADAR camera. The camera function was fulfilled with two boards inside. The APD readout board, where the SCA is mounted, has the FPGA and all the circuits for signal process and communication with the host processor through CameraLink interface. The rear board provides all the power supplies and TEC controlling for both TECs in and out of the SCA. As shown on the rear panel, the camera is powered solely by a 28-V source. The constant current is about 0.7 A. Because most of the current is consumed by the TECs, the peak can reach 1.5 A when the TECs are tuned on.

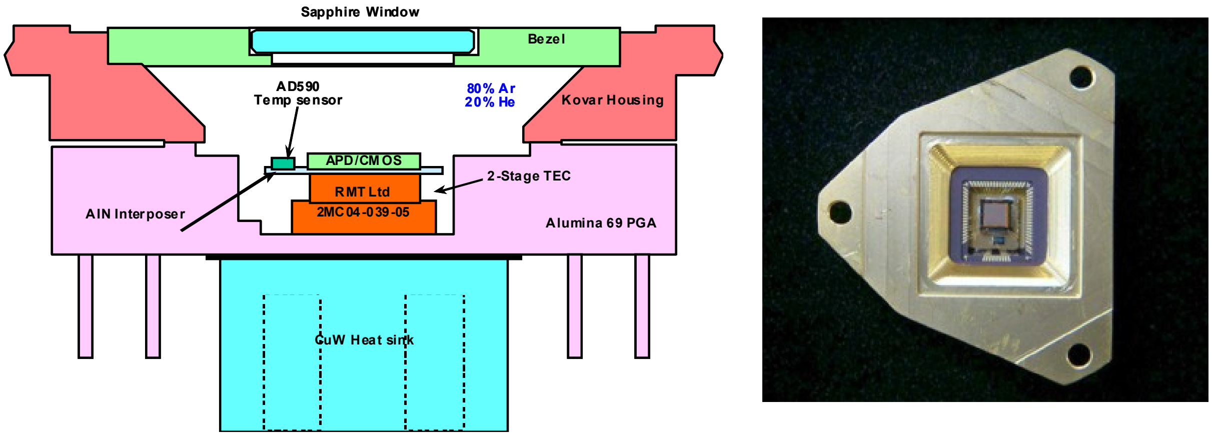

Figure 7. The crosssection and top view of a sensor chip assembly for Spectrolab Gen-I LADAR camera.

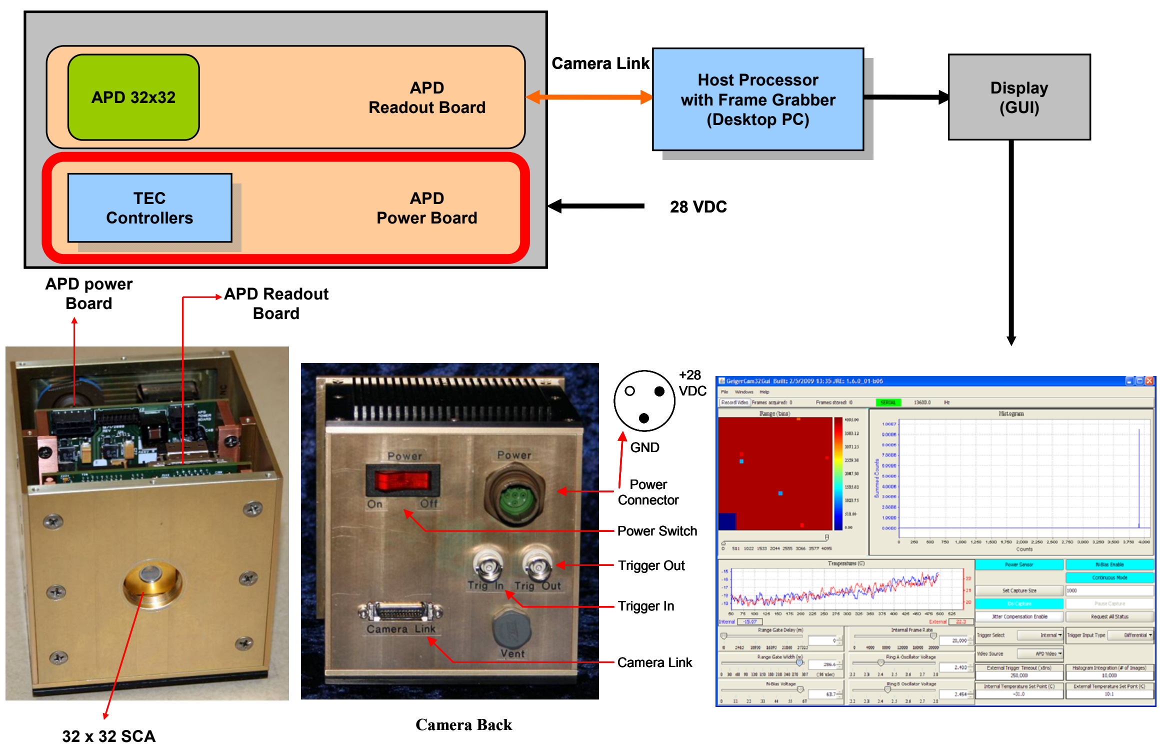

Figure 8. The pictures, block diagram, and controlling GUI of Spectrolab Gen-I LADAR camera.

Without any incident photon, we can get the DCR map of an SCA shown in the left panel of Figure 9. Most of the array demonstrates a DCR less than 20 kHz shown in deep blue. Because of the array non-uniformity in breakdown voltage, the lower right corner of the array is overbiased hard than the rest area, and shows a higher DCR in lighter blue. With an attenuated focused laser beam, we can get a spot image on the array, as shown in the right panel of Figure 9.

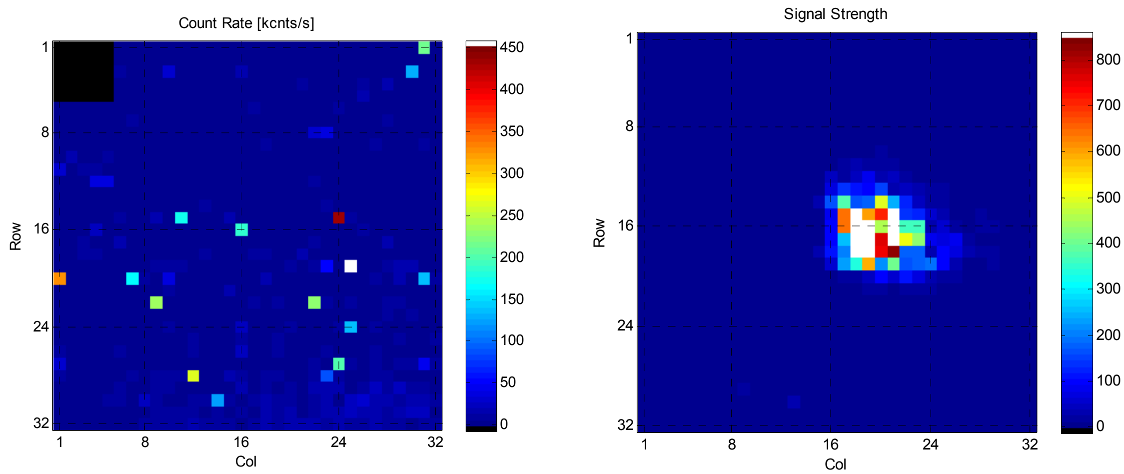

Figure 9. The DCR map and the photo response of a laser spot. The 5x5 area in upper left corner has a different circuit design in the CMOS 2002 ROIC for testing purpose, and these pixels do not operate as the rest of the array.

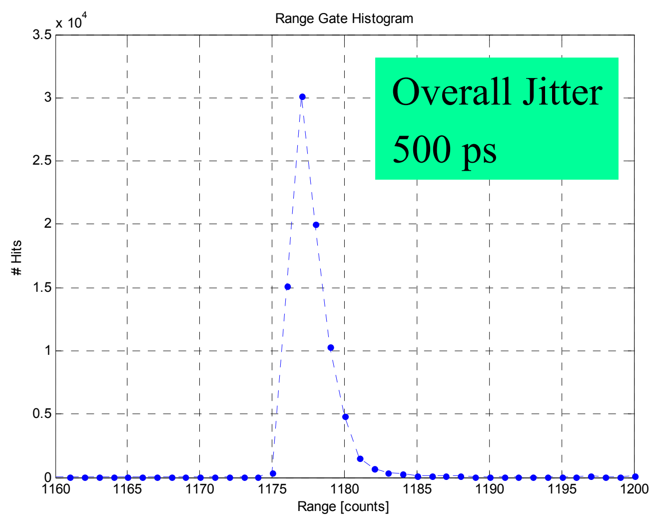

Figure 10. The temporal histogram of Spectrolab Gen-I LADAR camera to a synchronized 90ps laser pulse. The bin is 500ps wide, and the laser pulse width is included in this measurement. Based on the standard distribution of responses, the overall camera jitter is less than 1 bin, or 500 ps.

The ranging resolution of a LADAR camera is determined by its overall jitter performance. Figure 10 shows the temporal histogram of our Gen-I camera to a synchronized 90 ps laser pulse. The bin size is 500 ps, and the laser pulse width is included in this measurement. By calculating the standard deviation of this temporal distribution, we can get the overall camera jitter, which is less than 1 bin, or 500 ps.

The field demonstration is shown in the left panel of Figure 11. The picture is color coded with ranging information. In order to achieve a better lateral resolution, the camera mechanically scanned across the field and the images were stitched together. For comparison, the right panel shows a 2D picture taken from the same angle.

In summary, we integrated our 100-μm pitch 32x32 GM-APD arrays with CMOS 2002 ROICs designed by MIT-LL, and assembled them into SCAs for SWIR single-photon-level imaging applications. By integrating with readout and supporting circuits, we developed Spectrolab Gen-I LADAR camera. With 12-bit temporal resolution provided by CMOS 2002 ROIC, the operation gate can cover 2 μsec, with a resolution of 0.5 ns and a frame rate up to 20 kHz. The data download and command control are realized by a CameraLink connection in the base configuration. With a signal 28-V power supply, the power consumption is less than 20 W. Without the front lens, the camera weighs less than 5 lbs, and the volume is about 4.5”x4.5”x4.5”.

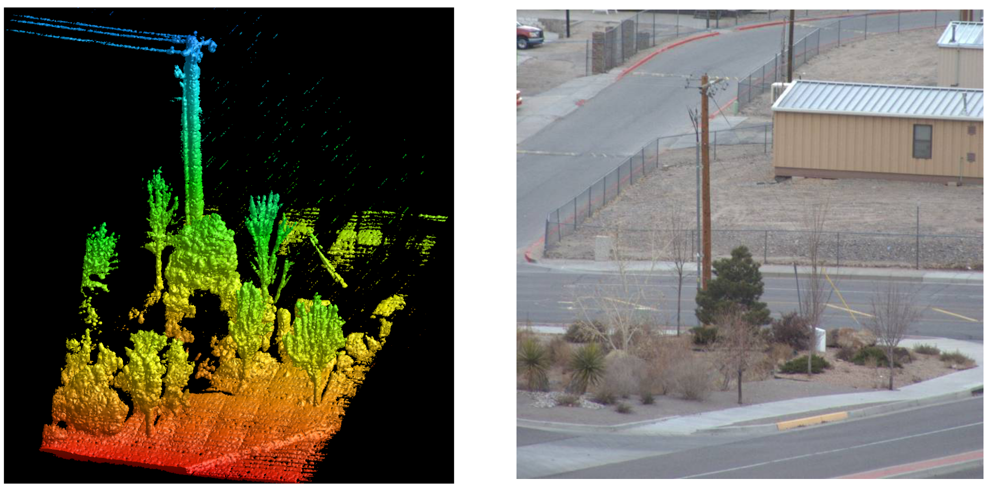

Figure 11. The 3D image taken with Spectrolab Gen-I LADAR camera. The picture is color coded with ranging information. The right panel shows the 2D image taken from the same angle.

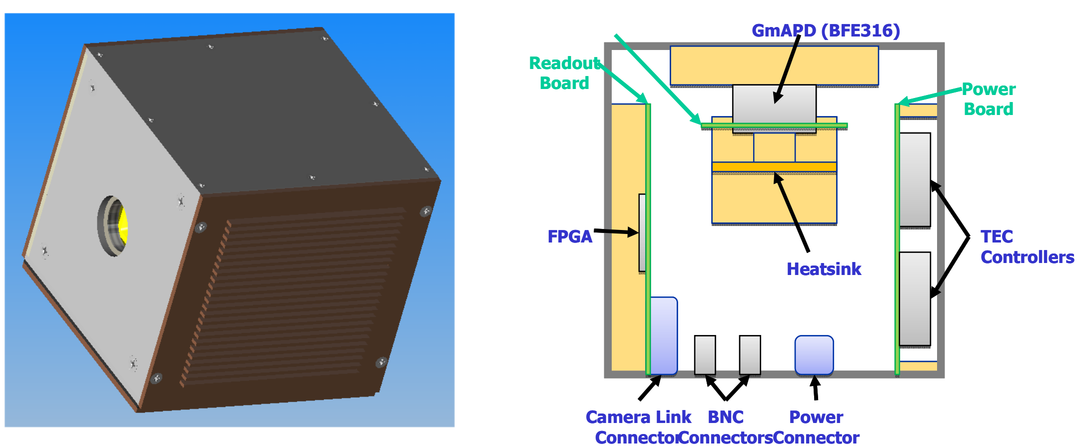

Figure 12 The mechanical design of Spectrolab Gen-II LADAR camera. The outside dimension is similar to that of Gen-I, but the internal arrangement will help to reduce the weight and power consumption.

5. SPECTROLAB GEN-II LADAR CAMERA

With the support from DARPA, a new readout-integrated circuit (ROIC), BFE316, was designed in 180-nm CMOS technology by Black Forest Engineering (BFE). This ROIC design is focused in improving the pixel functionality and minimizing the total timing jitter. By connecting the detector to a high impedance element, the front end circuit provides immunity to shorted detectors, which normally sparse in APD arrays, and thus greatly improves the manufacturability of FPAs. As shown in Figure 9, APD arrays have natural variations in breakdown voltage, which results in a performance variation across the array if it is biased under a uniform bias. By introducing a 4-bit in-pixel programmable NUB adjustment, the result SCA can achieve much better performance uniformity.

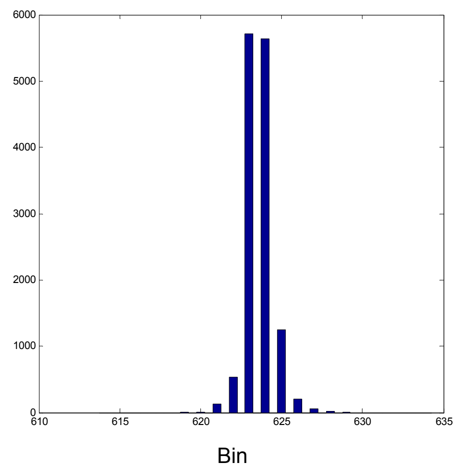

Figure 13. The measured timing jitter histogram of a GM-APD FPA, 9970-11-K14, with a BFE316 ROIC. Each bin corresponds to 500 ps. The timing jitter from these data is 435 ps.

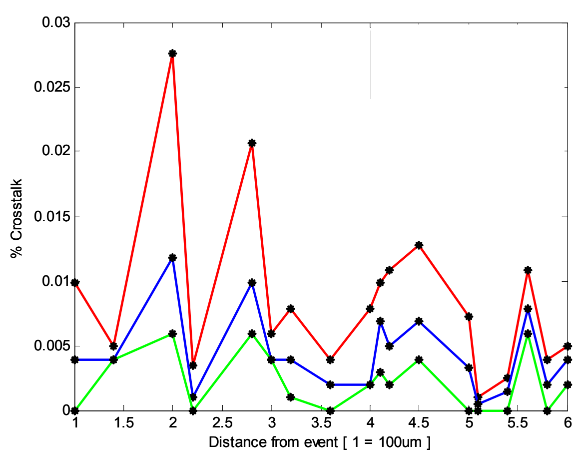

Figure 14. The measured cross talk at 240 °K as a function of position from an initial event as measured on FPA 9970-11-K14. Three separate durations after the event are shown: 0.5 ns, 1.0 ns, and 1.5 ns after the event.

For the 32x32 GM-APD arrays, most of the operation time is occupied by the data download and process. By using a SMIA data output protocol between the ROIC and the readout board, BFE 316 allows a frame rate up to 23 kHz. Similar to the Gen-I camera with CMOS 2002 ROIC, the Gen-II camera with BFE 316 will also utilize the

CameraLink connection for the communication between the host computer and the camera. With a single master input clock of 1 GHz, the same 0.5 ns time bin size will be maintained. As shown in Figure 13, stable time stamping makes the system demonstrate a time jitter about 435 ps. With a 14-bit timing resolution, the range-gates can be extended to > 6 μs from 2 μs as in the Gen-I camera, while maintaining the same minimum bin width. For the convenience in APD operations, the transient bias amplitude is increased to 14 V. Because ROIC is the major thermal load for the first TEC in a LADAR camera, the ROIC power consumption is critical to the whole camera power performance. Careful consideration was taken in the design of BFE316, and its power is limited to 300 mW in operation.

The new SCA follows the same structure as shown in Figure 7, but with a new ROIC, BFE 316, and an improved GM-APD array on P- InP substrate with higher PDE. As shown in Figure 12, the Gen-II camera uses a 3-board configuration, in which a smaller readout board is attached to the SCA and connected to the FPGA board by cables. The camera will have the same footprint as Gen-I but much less weight for its shorter heat path and less heat sinks.

The SCA assembly process is similar to that for the Gen-I camera. After integrating a 32x32 GM-APD array with a BFE316 ROIC chip, the FPA is packaged into hermetically-sealed modules and tested. The timing jitter was measured on pixels from SCA 9970-11-K14 with an array fabricated on a p-type substrate, and the timing histogram is shown in Figure 13. The array was operated at 4 V overbias and cooled to 240 K for these measurements. By calculating the standard deviation of the time distribution, the timing jitter was found to be 435 ps for this camera.

The crosstalk across the GM-APD arrays is shown in Figure 14. These data are analyzed from the DCR data where an initial Geiger event is correlated to subsequent events at surrounding pixels. The correlation period is varied to insure that cross talk is accurately determined. There is a clear geometric pattern consistent with an optical crosstalk mechanism. The number of events also increases with duration after the event. With an improved APD array design, the measured crosstalk is consistently less than 0.05%.

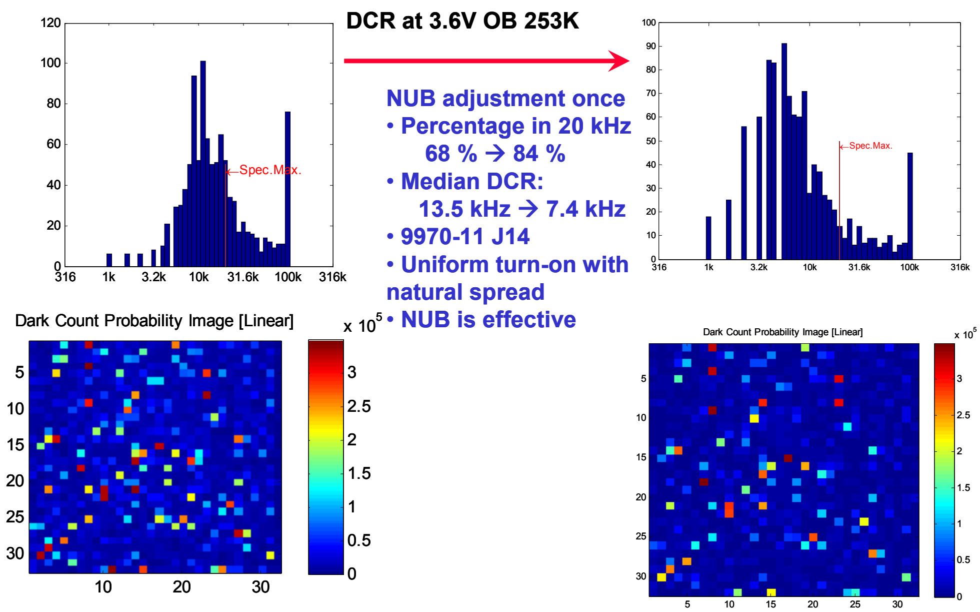

Figure 15 An example of the impact of non-uniform bias control on FPA DCR.

The impact of the NUB control is shown in **Figure 15**. By reducing the overbais of the hot pixels, the ones with high dark counts, one iteration of the algorithm to tune the NUB resulted in almost a 2x reduction in median dark counts of the 32x32 FPA with a BFE316 ROIC.

6. SUMMARY

To answer the challenges of SWIR LADAR applications, Spectrolab, together with Boeing SVS and Black Forest Engineering, has been developing GM-APD sensors and cameras. Continuous effect in improving in materials, device design and process has resulted in excellent FPA performance for LADAR sensors. Black Forest Engineering has designed and tested a new 32x32 ROIC specifically developed for LADAR FPAs. The integration effort at Boeing SVS finally made the cameras convenient to operate and commercially available. After developing two generations of 32x32 LADAR cameras, the Spectrolab and Black Forest Engineering team, are presently under contract to DARPA to develop and demonstrate a 128x32 format FPA for 1.06 µm applications.

ACKNOWLEDGEMENTS

We would like to acknowledge the invaluable assistance provided by MIT Lincoln Laboratory over the last several years under various technology transfer programs. This effort has been funded under Boeing Whitespace program and DARPA Elusive Surface Target Engagement Technology contract HR0011-08-C-0020 under the direction of Dr. Monte Turner.

REFERENCES

[1] K. A. McIntosh, et al., "Arrays of III-V semiconductor Geiger-mode avalanche photodiodes," Lasers and Electro-Optics Society, 2003. LEOS 2003. The 16th Annual Meeting of the IEEE. Volume 2, 686 (2003).

[2] R. Sudharsanan et al., "Single photon counting Geiger Mode InGaAs(P)/InP avalanche photodiode arrays for 3D imaging," Proc. SPIE 6950, 69500N-1 (2008).

[3] P. Yuan, R.Sudharsanan, J. Boisvert, X. Bai, P. McDonald, T. Isshiki, W. Hong, M. Salisbury, C. Hu, M. Liu, and J. C. Campbell, " High performance InP Geiger-mode SWIR avalanche photodiodes," Proc. SPIE 7320, 73200P (2009).

[4] S. Verghese, et al., "Arrays of InP-based Avalanche Photodiodes for Photon Counting," IEEE J. Selected Topics in Quantum Electronics, 13, 870 (2007).

[5] L. P. Gonzalez, J. M. Murray, S. Krishnamurthy, and S. Guha, "Wavelength dependence of two photon and free carrier absorptions in InP," Opt. Express **17**, 8741-8748 (2009).